water

MDPI

Article

Quantitation of Rainfall Retention Capacity for Small Reservoirs Considering Spatial Soil Moisture

Bingxing Tong [1,*], Yubin Chen [1], Yinshan Xu [1], Xiao Zhang [1] and Yufeng Ren [2]

[1] Bureau of Hydrology, Changjiang Water Resources Commission, Wuhan 430010, China; chenyb@cjh.com.cn (Y.C.); yinshanxu@163.com (Y.X.); zhangx@cjh.com.cn (X.Z.)
[2] China Yangtze Power Co., Ltd., Yichang 443000, China; thierry_ren@163.com
* Correspondence: 15295563139@163.com; Tel.: +86-27-8282-0171

Abstract: To realize the estimation of rainfall retention capacity for small reservoirs considering spatial soil moisture, a rainfall retention capacity model and its parameter schemes have been developed in this study. An iterative trial solution method considering potential rainfall and soil moisture for the model constructed was proposed for efficient computation. The rainfall retention capacity of 32 pilot small reservoirs located in ungauged basins of Hunan province was calculated starting from 21 August 2023. In addition, a continuous calculation was carried out from 1 August to 30 September 2023 using the proposed method for Heping reservoir. The results show that the Pearson's correlation coefficients between rainfall retention capacity and available reservoir capacity and soil moisture, are 0.36 and −0.64, respectively. Using Heping reservoir as an example, this study effectively characterized the dynamic change in its rainfall retention capacity, which ranged from 123.6 mm to 68 mm in August 2023. The analysis indicates the rainfall retention capacity of the pilot small reservoirs calculated is reasonably related to the soil moisture, supporting risk visualization for small reservoirs within rain-affected regions. Furthermore, the impact of the antecedent precipitation on rainfall retention capacity can also be dynamically quantified in real time, which provides reference for the continuous management of small reservoirs.

Keywords: small reservoirs; rainfall retention capacity; ungauged region; iterative trial calculations; Hunan province

check for updates

Citation: Tong, B.; Chen, Y.; Xu, Y.; Zhang, X.; Ren, Y. Quantitation of Rainfall Retention Capacity for Small Reservoirs Considering Spatial Soil Moisture. *Water* **2024**, *16*, 3114. https://doi.org/10.3390/w16213114

Academic Editor: Francesco De Paola

Received: 16 September 2024
Revised: 18 October 2024
Accepted: 22 October 2024
Published: 31 October 2024

Copyright: © 2024 by the authors. Licensee MDPI, Basel, Switzerland. This article is an open access article distributed under the terms and conditions of the Creative Commons Attribution (CC BY) license (https://creativecommons.org/licenses/by/4.0/).

1. Introduction

According to the China water development report 2023, as of the end of 2022, there were a total of 93,390 small reservoirs in China, accounting for 94.7% of the total number of reservoirs [1]. The safety of a considerable number of small reservoirs during the flood season represents a significant challenge, particularly in regions where there is a paucity of hydrological observation data. This pertinent issue has long been addressed by Predictions in Ungauged Basins (PUB), the most recent initiative of the International Association of Hydrological Sciences, producing a significant output in terms of community flood risk control. However, in rural areas of China lacking in hydrological monitoring, the world's largest group of small reservoirs becomes a Sword of Damocles threatening the lives and property of local people during heavy rains due to its low engineering design safety standards, small scale, and lack of maintenance. In recent years, the Chinese government has implemented a series of measures with the objective of enhancing the safety management of reservoirs and improving the country's flood prevention capacity. Among these measures, the quantitative analysis of flood risk of small reservoirs within ungauged regions represents a significant challenge [2,3].

The rainfall retention capacity, a potentially key indicator in the quantification of flood risk in small reservoirs, is defined as the maximum amount of rainfall that can be accommodated during a given period, taking into account a range of factors including

the reservoirs' operation and the hydrological characteristics of the underlying surface of the watersheds [4,5]. The research topic of calculating the rainfall retention capacity of small reservoirs has drawn attention from many researchers. Hou et al. contemplated the antecedent precipitation index, the existing water levels in the reservoir, and the operation of the reservoir, facilitating a reasonable estimation of the rainfall retention capacity [6]. A comprehensive review of the calculation methods for the rainfall retention capacity of small reservoirs was provided by Zhang et al., offering examples of how to quantify the impact of rainfall and the operation of water projects in their calculations [7]. Yuan et al. developed models for reservoir capacity estimation based on statistical and machine learning algorithms for national-scale reservoirs in China [8]. Nevertheless, there is a scarcity of comprehensive and rigorous research examining the rainfall retention capacity of small reservoirs in ungauged regions [9].

This study addresses the challenge of parameter calibration for a rainfall retention capacity model for small reservoirs, which is typically hindered by a lack of empirical data and measurements. A computational model for rainfall retention capacity, adaptable to the diverse operational modes of small reservoirs, has been constructed. The influences of potential rainfall and the characteristics of the watershed's underlying surface on the model parameters have been comprehensively quantified. An iterative trial method for calculating the rainfall retention capacity, which takes into account various rainfall scenarios during the forecast period, has been developed. As a case study, rapid batch calculations of rainfall retention capacity were conducted for 32 pilot small reservoirs in Hunan province, thereby validating the rationality and applicability of the proposed model.

2. The Study Area

Hunan province is characterized by a network of four principal rivers, namely the Xiang Jiang, Zi Shui, Yuan Shui, and Li Shui Rivers. These water courses follow a south-to-north trajectory, ultimately merging into Dong Ting Lake, thereby constituting a comprehensive hydrological system. This system encompasses 5341 rivers with a flow length exceeding 5 km, collectively extending to a total length of 90,000 km. The calculation in this study involves 32 small reservoirs, primarily situated in Shi Men County, Xiang Xiang City, and Liu Yang City (Figure 1).

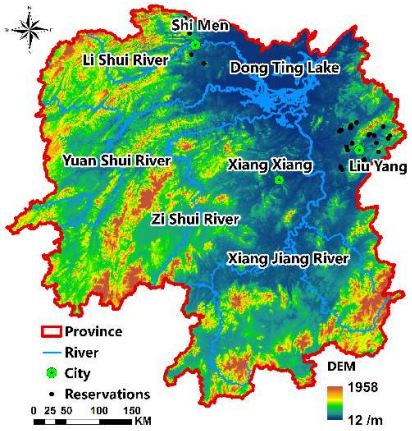


Figure 1. Topography, the water system, and small reservoirs within Hunan province.

3. Materials and Methods

3.1. Materials

Basic information such as characteristic water levels, watershed areas, dam heights, and spillway elevation was primarily collected for 32 pilot reservoirs in Hunan province. Given the recent installation of monitoring equipment and the limited amount of monitoring data available for the pilot small reservoirs, the data selected for this study primarily include hourly water level records from June 2023 onwards. Additionally, the measured

rainfall was sourced from ground observation stations, while the numerical rainfall prediction data were obtained from the European Centre for Medium Range Weather Forecasts (ECMWF) [10].

3.2. Methods

3.2.1. Estimation of Rainfall Retention Capacity in Various Reservoir Operation Scenarios

In this study, the amount of rainfall necessary to elevate the current water level of the reservoir to the spillway bottom is preliminarily calculated. Following this, analysis of the rainfall scenarios within the forecast period is conducted to assess whether the reservoir would activate the operation of spillway facilities. Additionally, the impact of reservoir spillway operations on rainfall retention capacity needs to be considered. Furthermore, the dynamic runoff coefficient is taken into account, thus enabling reasonable calculation of rainfall retention capacity applicable to various reservoir operation stages.

(a) Calculation of rainfall retention capacity without reservoir discharge

In the circumstance that the water level is below the reservoir spillway, calculation determining the available storage capacity of the reservoir below this elevation has been carried out. Subsequently, this storage capacity is converted into the rainfall over the watershed by incorporating the runoff coefficient, enabling the computation of the rainfall retention capacity without reservoir discharge (Equation (1)).

$$P_{cx} = k_{\mathrm{c}} \frac{(W_{z_1} - W_{z_0})}{\alpha F} \tag{1}$$

where P_{cx} is the rainfall retention capacity when the water level of the reservoir is below the reservoir spillway, mm; W_{z_1} is the reservoir storage capacity corresponding to the spillway elevation, m^3; W_{z_0} is the corresponding reservoir storage capacity at the current water level Z_0, m^3; F is the watershed area, km^2; α is the runoff coefficient; and k_{c} is the unit conversion factor.

(b) Calculation of rainfall retention capacity considering reservoir discharge

During the reservoir's actual operation, when the water level exceeds the spillway, the influence of reservoir discharge on the calculation of rainfall retention capacity must be considered. In such scenarios, the corresponding discharge rate at a given water level is determined by the curve of water release and simultaneously estimation of the duration of discharge. Subsequently, the total discharge volume is added to the available storage capacity, and the combined volume is then converted into an equivalent amount of rainfall, which represents the rainfall retention capacity considering reservoir discharge.

If the current water level is lower than the bottom of the spillway, the formula for calculating the rainfall retention capacity is shown in Equation (2).

$$P_{cs} = k_c \frac{(W_{z_1} - W_{z_0})}{\alpha_1 F} + k_c \frac{(W_{z_2} - W_{z_1})}{\alpha_2 F} + m \frac{Q_{ave} \times \Delta t}{\alpha_2 F} \tag{2}$$

where P_{cs} is the rainfall retention capacity that will raise the water level to a target level, which is above the elevation of the spillway's bottom, mm; W_{z_2} is the corresponding reservoir capacity at the target flood level Z_2, m^3; Q_{ave} is the average discharge of the reservoir, m^3/s; Δt is the duration of discharge, h; α_1 is the average runoff coefficient when the water level rises from the current water level to the spillway's bottom; α_2 is the average runoff coefficient; and m is the unit conversion factor.

The duration of reservoir discharge Δt can be estimated from the rainfall P_1 during the water level rise from Z_0 to Z_1 and the total rainfall P_{sum} of the forecast period; Q_{ave} can be estimated based on the corresponding discharge rate at Z_2, which is higher than the elevation of the spillway (Equations (3) and (4)).

$$\Delta t = L \times \left(1 - \frac{P_1}{P_{sum}}\right) \tag{3}$$

$$Q_{ave} = 0.5 \times Q_2 \tag{4}$$

where L is the forecast period, h; Q_2 is the corresponding discharge rate at the design flood level, m^3/s.

If the current water level is higher than the bottom of the spillway, the formula for calculating the rainfall retention capacity is shown in Equation (5).

$$P_{xs} = k_c \frac{(W_{z_2} - W_{z_1})}{\alpha_2 F} + m \frac{Q_{ave} \times L}{\alpha_2 F} \tag{5}$$

$$Q_{ave} = 0.5 \times (Q_0 + Q_2) \tag{6}$$

where Q_0 is the discharge flow rate corresponding to Z_0, m^3/s.

3.2.2. Estimation of Initial Soil Moisture

The rainfall retention capacity is closely related to runoff generation, which exhibits a significant positive correlation with the initial soil moisture. In this study, the soil water storage capacity in the watersheds was first estimated using refined soil texture data, and then, based on the theory of saturation excess runoff generation, dynamic calculation of the soil moisture at the daily scale was conducted 30 days in advance using rainfall and evapotranspiration as the inputs to obtain the soil moisture at the time at which the rainfall retention capacity was calculated. The soil texture data were provided by SoilGrids version 2.0, which produces maps of soil properties for the entire globe at a medium spatial resolution of a 250 m cell size using machine learning methods. It takes as input soil observations from approximately 240,000 locations worldwide and more than 400 global environmental covariates describing vegetation, terrain morphology, climate, geology, and hydrology [11–13].

The estimated soil water storage capacity of the watersheds is given by Equation (7).

$$W_m = L_a \times \left(\theta_{fc} - \theta_{wp}\right) \tag{7}$$

where W_m represents the soil water storage capacity, mm; θ_{fc} represents the field capacity; and θ_{wp} represents the wilting point, and these variables can be calculated based on the soil texture data provided by SoilGrids.

Based on field investigations, it is considered that the maximum vadose zone thickness $L_{a,max}$ within the watershed occurs near the ridge, which is taken as the upper limit for estimating the spatial distribution of the vadose zone thickness, while the vadose zone thickness near the riverbank is taken as the lower limit. Between the riverbank and the ridge, the spatial distribution of the vadose zone thickness is estimated based on the watershed topographic index [14] and the soil thickness data provided by SoilGrids (Equation (8)).

$$L_a = L_{a,max} \times e^{\left(-\frac{lnTI}{\delta}\right)^{\epsilon}} \tag{8}$$

where L_a is the estimated vadose zone thickness, mm; TI is the topographic index; and δ and ϵ are parameters that can generally be taken as 2 and 4.6 [15,16], respectively. In practical applications, adjustments can be made to these parameters according to the specific surface characteristics of the watershed and experience in flood simulation.

The soil's hydrologic properties, including field capacity (θ_{fc}) and wilting point (θ_{wp}), can be calculated using the soil texture data provided by SoilGrids [16–18]. Once the parameter W_m is established, soil moisture W could be calculated based on rainfall and evapotranspiration as the inputs using the saturation excess runoff model.

3.2.3. Iterative Calculation of Rainfall Retention Capacity Considering Potential Rainfall

The runoff coefficient, the critical parameter in a rainfall retention capacity model, is subject to real-time changes during rainfall events, which makes it challenging to accurately determine the average runoff coefficient over a forecast period [17–19]. Therefore, in this study, an iterative calculation method for solving the rainfall retention capacity was proposed (Figure 2). First, it estimates an initial value for the rainfall retention capacity based on the soil moisture of the watershed. Subsequently, incorporating the runoff coefficient, an iterative solution process is conducted to determine the rainfall retention capacity. The steps are as follows:

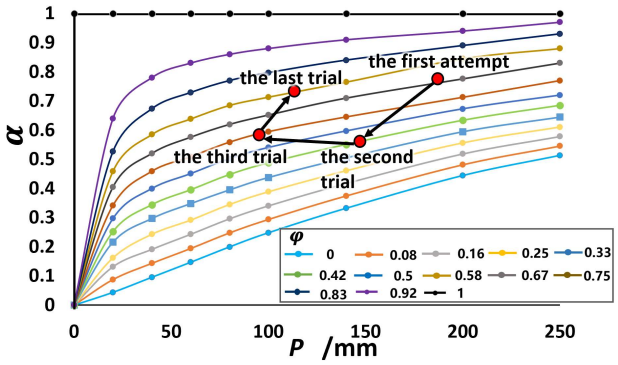


Figure 2. Illustration of the iterative trial calculation for rainfall retention capacity considering the time-varying runoff coefficient.

(a) The initial value, P_{Ic}, for the trial calculation of the rainfall retention capacity is obtained by incorporating the maximum water storage capacity of the watershed, W_m, (Equation (9)).

$$P_{Ic} = W_m - W + k_c \frac{(V_{z_1} - V_{z_0})}{F} \tag{9}$$

(b) Based on the initial value P_{Ic}, the corresponding runoff coefficient α_c is determined using the functional relationship between precipitation (P), soil moisture saturation (φ), and the runoff coefficient. It is noteworthy that when calculating the runoff coefficient, the future rainfall should be set in order to account for the change in the runoff coefficient during the forecast period. Then, using the method provided in Section 3.2.1 and with the known parameters α_c and the operation mode of the reservoir, P_{cx} is calculated.

(c) Calculate the difference, which is denoted by ΔP_c, between P_{cx} and P_{Ic} in order to commence the subsequent iterative trial calculation (Equation (10)).

$$\Delta P_c = |P_{cx} - P_{Ic}| \tag{10}$$

Updating the initial value of P_{Ic} will be triggered when ΔP_c is greater than the threshold (Equations (11) and (12)).

$$P_{Ic,n+1} = P_{Ic,n} - 0.5 \times \Delta P_{c,n} \; if \; P_{cx,n} < P_{Ic,n} \tag{11}$$

$$P_{Ic,n+1} = P_{Ic,n} + 0.5 \times \Delta P_{c,n} \; if \; P_{cx,n} > P_{Ic,n} \tag{12}$$

where n represents the number of iterative trial calculations.

If the value of ΔP_c is less than the threshold, the corresponding value P_{cx} is taken as the final result of the trial calculation, with the threshold value for the trial calculation generally set at 3 mm.

4. Results and Discussion

4.1. The Parameter Scenarios for Rainfall Retention Capacity Models Within Ungauged Regions

The principal parameters of the rainfall retention capacity model are presented in the Table 1.

Table 1. Parameters for the rainfall retention capacity model.

Parameters	Meaning of Parameters	Unit	Parameters	Meaning of Parameters	Unit
Z-Qout	Discharge curve		α	Runoff coefficient	
Z-V	Storage capacity curve of the reservoir		F	Area	km^2
Zs	Design flood level	m	k_c	Unit conversion factor	
Zx	Flood control water level	m	L	Anticipation period	h

As defined in the Standard for Essential Technical Terms and Symbols in Hydrology (GB/T50095-2014) [20], the runoff coefficient represents the ratio of the average runoff depth of a watershed over a specified period to the corresponding rainfall, which is a crucial parameter quantifying flow production.

Taking into account that the runoff coefficient is mainly influenced by rainfall and soil moisture saturation, this study focuses on the functional relationship between rainfall (P), soil saturation (φ), and the runoff coefficient (α) as the core parameters of the model. In accordance with Hunan province's rainstorm and flood calculation manual [21], the hydrological zones are identified. In each hydrological zone, the relationship between rainfall, antecedent precipitation, and runoff is generalized into a three-variable correlation curve (P-P_a-R), which can be used as a reference to further determine the curve between P, φ, and α.

4.1.1. Hydrological Zones Within Hunan Province

Within the hydrological zones, the soil water storage capacity (W_m) and maximum watershed loss volume (I_o) are presented in Figure 3 and Table 2.

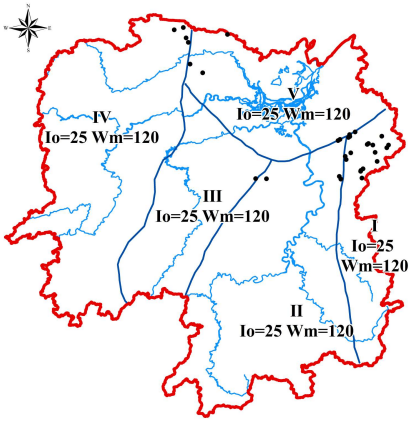


Figure 3. Hydrological zones within Hunan province.

Table 2. Functions between rainfall and runoff coefficient in Hunan province.

Hydrological Zones	Function	P/mm	W_m/mm	I_o/mm
I	$\alpha = 1 - 21/P$	>110	110	21
II	$\alpha = 1 - 32/P$	>120	120	32
III	$\alpha = 1 - 27/P$	>110	110	27
IV	$\alpha = 1 - 25/P$	>120	120	25
V	$\alpha = 1 - 35/P$	>116	116	35

The parameter I_o is used to describe the maximum amount of water loss before surface runoff occurs. These losses may encompass reductions in water volume caused by evaporation, infiltration, or surface runoff, as well as declines in groundwater levels. Analysis of the parameter I_o reveals the characteristics of runoff generation within a watershed. To summarise, within regions II and V with lower values of parameter I_o, the soil would be saturated more easily, which are more prone to flow production.

4.1.2. Function Between the Runoff Coefficient and Rainfall

The relationship between rainfall and the runoff coefficients can be visualized according to the schedules in the manual for calculating rainstorms and floods in Hunan province (Figure 2). As rainfall persists, the vadose zone gradually becomes saturated, and the amount of rainfall loss within the catchment no longer increases significantly. At this point, the rainfall loss is approximately equal to the value of parameter I_o, and thereafter a stable function is established between the runoff coefficient and cumulative rainfall (Table 2).

4.1.3. The Construction of Parameter Schemes for Reservoirs Within Ungauged Regions

The P-P_a-R curves of the Gao An, Wan Jia Bu, Ge He Yan, and Gao Ba Zhou stations should be synthesized and combined with the manual for calculating rainstorms and floods in Hunan province in order to refine the P-P_a-R curves for Shi Men County (Area1 in Figure 4) and Liu Yang City (Area2 in Figure 4). First, a series of rainfall amounts are set, and the functional relationship in Table 2 is utilized to calculate the combinations of rainfall and the runoff coefficient [P_n, $\alpha_{s,n}$], which are defined as the reference points highlighted in red in Figure 5. On the referenced P-P_a-R curve, the runoff coefficient $\alpha_{c,n}$ is calculated with the same antecedent precipitation as those of the reference points. Subsequently, the ratio between $\alpha_{s,n}$ and $\alpha_{c,n}$ is calculated, and the mean value β of multiple calculations is obtained, which is then employed to multiply the nodes of the transplanted P-P_a-R curve.

The ratio of R to P (denoted as α) is plotted on the vertical axis, with P on the horizontal axis. The ratio of Pa to Im in the region of the small reservoir is calculated as a third variable, soil moisture saturation φ. Furthermore, the functional relationship between precipitation (P), the runoff coefficient (α), and soil moisture saturation (φ) can be quantified (Figure 5).

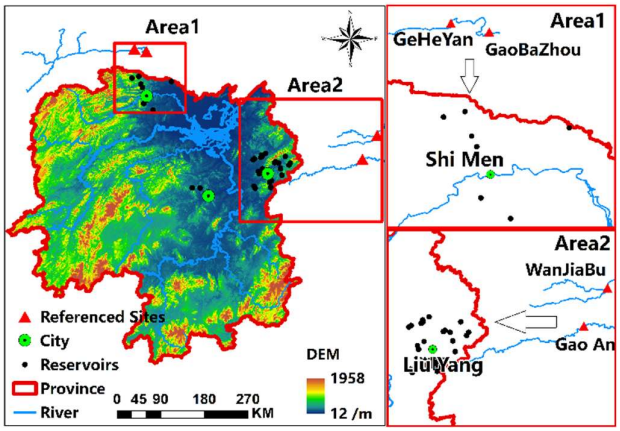


Figure 4. Parameter scheme transplantation.

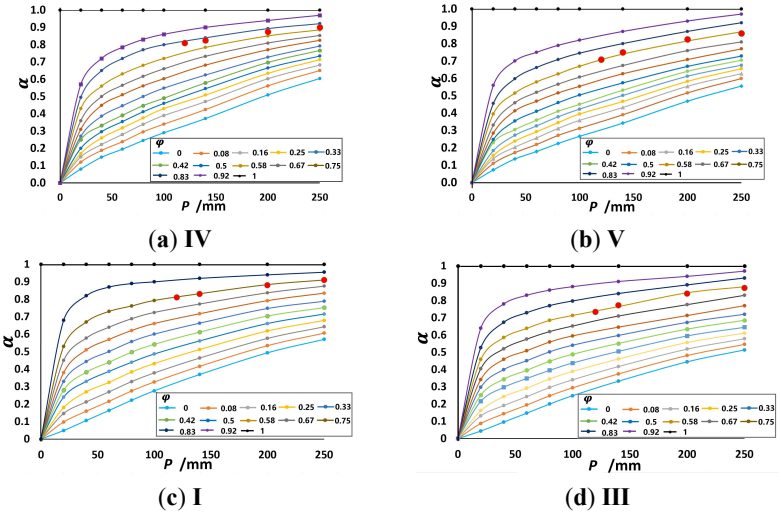


Figure 5. The optimized functional relationship among P, φ and α.

4.2. Estimation of Soil Moisture

To update the values of soil saturation, the spatiotemporal dynamics of soil moisture need to be simulated during the rainfall process. In this study, the Grid-Xin'anjiang model [22], using several orthogonal grids as computational units, is employed to simulate the spatiotemporal dynamics of soil moisture. This process first requires the spatial distribution of the soil's physical properties, such as saturated water content and field capacity (Figure 6), to be estimated based on SoilGrids [23].

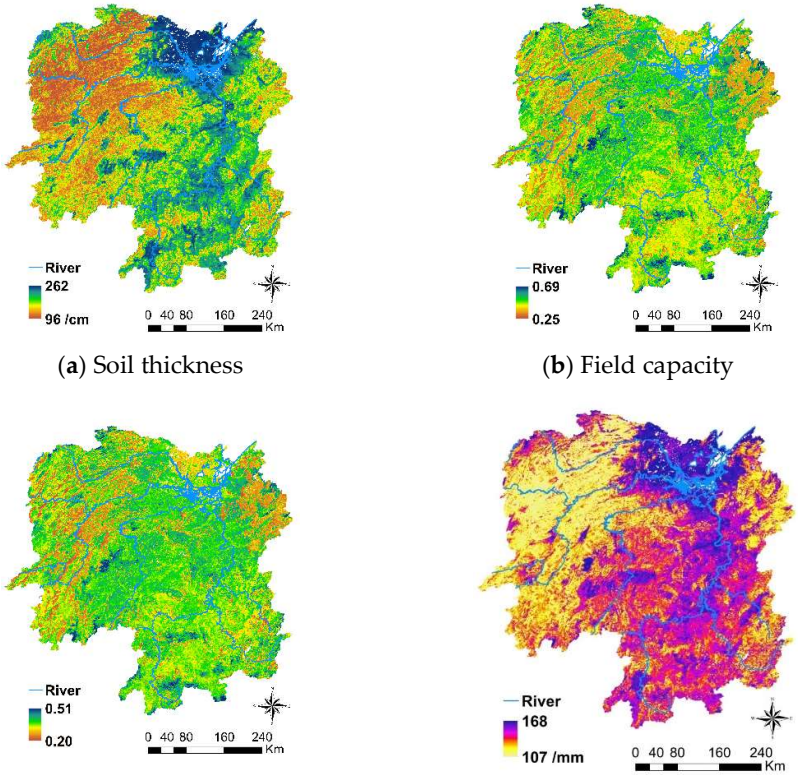
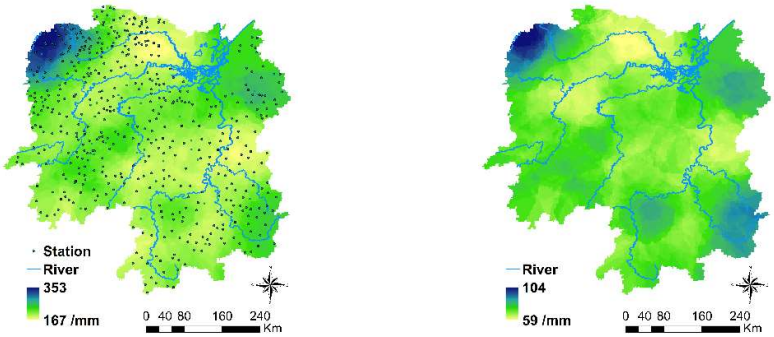


Figure 6. Spatial soil physical properties in Hunan province.

We set a preheating period of 45 days; use the spatial distribution of rainfall obtained through inverse distance weighting interpolation of the observational data from rain gauge

stations within Hunan province as the input; and thereby obtain the spatial soil moisture on 21 August 2023 (Figure 7).



(**a**) (**b**)

Figure 7. Spatial rainfall and soil moisture in Hunan province. (**a**) The spatial accumulated rainfall during the preheating period. (**b**) The spatial soil moisture.

4.3. Flood Risk Estimation Using Rainfall Retention Capacity Model

4.3.1. The Spatial Distribution of Rainfall Retention Capacity

The rainfall retention capacity of the small reservoirs was obtained through rolling calculations, with 21 August 2023 as the starting time. This was then compared with the numerical rainfall forecast from ECMWF to quantify the flood risk (Figure 8).

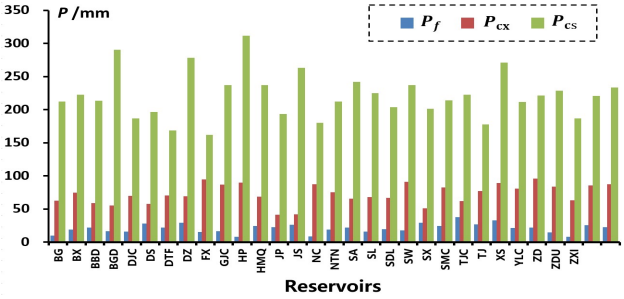
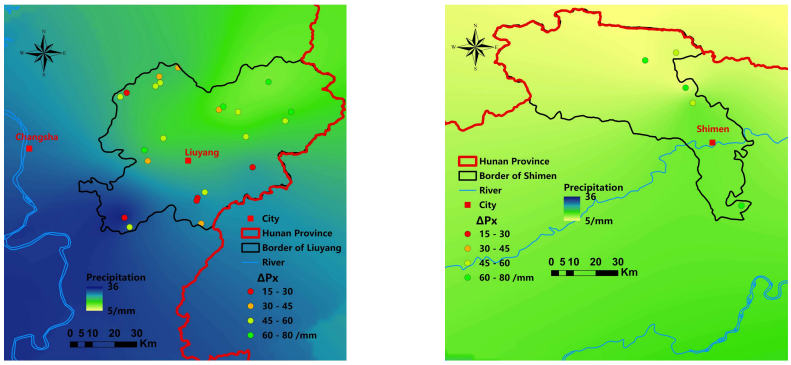


Figure 8. Calculated rainfall retention capacity for small reservoirs. (P_f represents the forecasted rainfall, and P_{cs} and P_{xs} represent the rainfall retention capacity in different situations, as detailed in Equations (2) and (5)).

It can be observed that the calculated rainfall retention capacity is greater than the rainfall during the entire forecast period. This indicates a low probability of issuing warnings due to reservoir water level changes during the forecast period. The difference (denoted as ΔP_x) between the rainfall retention capacity and the numerical rainfall prediction was calculated to reflect the flood risk of the reservoirs. An elevated value for ΔP_x signifies a decreased likelihood of flooding, whereas a diminished value points to a heightened risk. The distribution of ΔP_x of the pilot reservoirs is shown in Figure 9, which makes it obvious that the forecast rainfall is concentrated in the Liu Yang region during the 21–22 August 2023 period. Therefore, these small reservoirs face heightened vulnerability to flooding. In comparison, the expected future precipitation for the reservoirs, situated within Shi Men County, is relatively low, with ΔP_x values exceeding 60 mm, which indicates the minimal risk of flooding in these reservoirs. It can be concluded that the method proposed in this study offers an intuitive representation of the flood risk distribution of small reservoirs, thereby providing valuable support for flood prevention and dynamic control of risk.



(**a**) Liu Yang City (**b**) Shi Men County

Figure 9. The spatial distribution of rainfall retention capacity.

4.3.2. Estimated Flood Risk of Small Reservoirs

In addition to an overall understanding of the flood risk associated with small reservoirs, tracking dynamic changes in rainfall retention capacity is also essential in early flood warnings for small reservoirs. The rainfall retention capacity of Heping reservoir in Shi Men County has been continuously calculated from 1 August to 30 September 2023. Furthermore, the correlation between rainfall retention capacity and water level, as well as the antecedent precipitation index, has been analyzed (Figures 10 and 11).

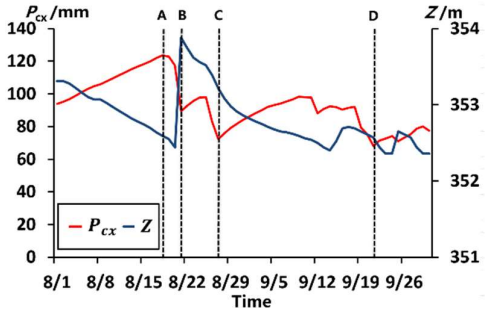


Figure 10. Dynamic rainfall retention capacity and water level of Heping reservoir.

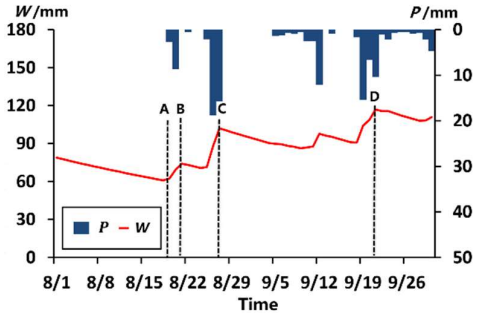


Figure 11. The soil moisture of Heping reservoir's watershed varying with the rainfall process.

The times indicated in Figures 10 and 11, labeled A, B, C, and D, and the corresponding rainfall retention capacity, water levels, and antecedent precipitation index are presented in Table 3.

Table 3. Rainfall retention capacity, water level, and antecedent precipitation index at various time nodes.

Point	Time	Rainfall Retention Capacity/mm	Water Level/m	Soil Moisture/mm
A	18 August	123.6	352.59	60.9
B	21 August	89.4	353.88	74.0
C	27 August	72.4	353.21	102.0
D	21 September	68.0	352.57	116.8

Before 18 August, there was no rainfall in the area of Heping reservoir, causing the soil moisture to continuously decrease to 10.6 mm, with soil moisture saturation at approximately 0.5. Consequently, the calculated rainfall retention capacity continued to increase, reaching a high point of 123.6 mm on August 18th. Although the soil moisture only increased slightly, by about 13 mm, the reservoir's water level increased rapidly, with a rise of 1.3 m, resulting in a rapid decline in the reservoir's rainfall retention capacity to 89.4 mm on 21 August. From 22 August to 27, the soil moisture increased to a peak of 102 mm due to rainfall, with soil moisture saturation at approximately 0.84, and the rainfall retention capacity calculated was reduced to 72.4 mm. From 27 August to 21 September, there were two consecutive rainfall events, and the soil moisture climbed to 116.8 mm. However, due to the fluctuating decline in the reservoir's water level, the rainfall retention capacity on 21 September was 68 mm, showing a small change compared to 27 August.

It can thus be seen that the rainfall retention capacity of the reservoirs calculated in this manuscript reflects the combined effects of the reservoir's water level and the soil moisture. This not only allows for assessment of flood control risk for small reservoirs but also considers the dynamic impacts of the water levels of reservoirs and the expected future precipitation on the rainfall retention capacity in real time.

5. Conclusions

This study addresses the issue of early warnings for small reservoirs within ungauged regions by constructing a rainfall retention capacity model applicable to different reservoirs' operation. The impacts of rainfall and the underlying surface characteristics on the parameter scheme are quantified comprehensively, and an iterative calculation method considering the expected future rainfall has been developed. This method is used to calculate the rainfall retention capacity of 32 pilot small reservoirs in an ungauged region of Hunan province, with 21 August 2023 as the starting time.

The results show that the Pearson's correlation coefficients between rainfall retention capacity and available reservoir capacity and soil moisture are 0.36 and -0.64, respectively. Using Heping reservoir as an example, this study effectively characterized the dynamic change in its rainfall retention capacity, which ranged from 123.6 mm to 68 mm in August 2023. The analysis indicates the rainfall retention capacity of the pilot small reservoirs calculated is reasonably related to the soil moisture, supporting risk visualization for small reservoirs within the rain-affected region. Furthermore, the impact of the antecedent precipitation on rainfall retention capacity can also be dynamically quantified in real time, which provides reference for the continuous management of small reservoirs.

However, it must be acknowledged that some valuable work, such as comparison with other similar or close studies, was not included in this study. According to the schedul, these work would be conducted in further research with sufficient data. Simultaneously, drawing from the practical experience of this project, it was realized by the researchers that the methods developed must be adapted to characteristics such as the lack of observational data, the limited technical expertise of reservoir managers, and the extensive distribution of small reservoirs. This requires a delicate balance between computational accuracy and ease of replication, which is crucial for such research to be widely applied and to gather sufficient feedback to refine itself.

Author Contributions: Conceptualization, B.T. and Y.C.; methodology, Y.X. and B.T.; formal analysis, X.Z. and B.T.; investigation, B.T. and Y.X.; resources, Y.C.; data curation, B.T., Y.X. and Y.R.; writing—original draft preparation, B.T. and X.Z.; writing—review and editing, Y.C., Y.X. and Y.R.; visualization, B.T. and Y.X.; supervision, Y.C.; funding acquisition, Y.X. and Y.R. All authors have read and agreed to the published version of the manuscript.

Funding: This research was funded by the National Key Research and Development Program of China (Grant No. 2023YFC3209103); the National Key Research and Development Program of China (Grant Nos. 2023YFC3206001 and 2023YFC3206003); the National Natural Science Foundation of China (Grant Nos. 51679061 and 51979070); the Science and Technology Innovation 2024 Major Project of the Bureau of Hydrology, Changjiang Water Resources Commission (Grant No. SWJ-24CJX11); and the research project of China Changjiang Electric Power Co., Ltd. (Grant No. Z242302034).

Data Availability Statement: The data are unavailable due to privacy restrictions.

Conflicts of Interest: Author Yufeng Ren was employed by the company China Yangtze Power Co., Ltd. The remaining authors declare that the research was conducted in the absence of any com-mercial or financial relationships that could be construed as a potential conflict of interest. The authors declare that this study received funding from China Changjiang Electric Power Co., Ltd. The funder was not involved in the study design, collection, analysis, interpretation of data, the writing of this article or the decision to submit it for publication.

References

1. Ministry of Water Resources of the People's Republic of China. *China Water Development Report 2023*; China Water Power Press: Beijing, China, 2023.
2. Cao, S.; You, R.; Li, X.; Jia, J.; Wang, J.; Liu, Y. A novel approach for estimating the capacity of ungauged small reservoirs using remote sensing and DEM. *Hydrol. Res.* **2022**, *53*, 1001–1016. [CrossRef]
3. Kim, D.; Eum, H.I.; Kaluarachchi, J.J.; Chun, J.A. A sensitivity-based analysis for managing storage capacity of a small agricultural reservoir under drying climate. *Agric. Water Manag.* **2019**, *213*, 410–418. [CrossRef]
4. Verstraeten, G.; Leuven, K.; Poesen, J. Estimating trap efficiency of small reservoirs and ponds: Methods and implications for the assessment of sediment yield. *Prog. Phys. Geogr. Earth Environ.* **2000**, *24*, 19–51. [CrossRef]
5. Liebe, J.; Van De Giesen, N.; Andreini, M. Estimation of small reservoir storage capacities in a semi-arid environment: A case study in the Upper East Region of Ghana. *Phys. Chem. Earth* **2005**, *30*, 448–454. [CrossRef]
6. Hou, A.Z.; Hu, Z.D.; Zhu, B.; Wang, R.; Zhu, B.; Lu, H.J. Concept and calculation of small- and medium-sized reservoir's retaining capacity. *J. China Hydrol.* **2017**, *37*, 35–38.
7. Zhang, S.L.; Hou, A.Z.; Wu, Z.Y.; Yi, Z.J. *Research on Key Technology of Small and Medium Sized Reservoir's Retaining Capacity*; China Water Power Press: Beijing, China, 2019.
8. Yuan, C.; Liu, C.; Fan, C.; Liu, K.; Chen, T.; Zeng, F.; Zhan, P.; Song, C. Estimation of water storage capacity of Chinese reservoirs by statistical and machine learning models. *J. Hydrol.* **2014**, *630*, 130674. [CrossRef]
9. Liu, L.; Li, G.W.; Dong, F.F.; Zhang, Y.; Liu, G. Study on calculation methods of small and medium-sized reservoir's rainwater retaining capacity. *China Flood Drought Manag.* **2022**, *32*, 66–71.
10. Liu, L.; Feng, J.; Ma, L.; Yang, Y.; Wu, X.; Wang, C. Ensemble-based sensitivity analysis of track forecasts of typhoon In-fa (2021) without and with model errors in the ECMWF, NCEP, and CMA ensemble prediction systems. *Atmos. Res.* **2024**, *309*, 107596. [CrossRef]
11. Poggio, L.; De Sousa, L.M.; Batjes, N.H.; Heuvelink, G.B.; Kempen, B.; Ribeiro, E.; Rossiter, D. SoilGrids 2.0: Producing soil information for the globe with quantified spatial uncertainty. *Soil* **2021**, *7*, 217–240. [CrossRef]
12. Batchu, V.; Nearing, G.; Gulshan, V. A Deep Learning Data Fusion Model using Sentinel-1/2, SoilGrids, SMAP, and GLDAS for soil moisture retrieval. *J. Hydrometeorol.* **2023**, *24*, 1789–1823. [CrossRef]
13. Zhu, C.; Ding, J.; Zhang, Z. Soil salinity dynamics in arid oases during irrigated and non-irrigated seasons. *Land Degrad. Dev.* **2023**, *34*, 3823–3835. [CrossRef]
14. Qiu, A.N.; Zhang, Y.J.; Wang, G.X.; Cui, J.; Song, Y.X.; Sun, X.Y.; Chen, L. A modified TOPMODEL introducing the bedrock surface topographic index in Huangbengliu watershed, China. *J. Mt. Sci.* **2022**, *19*, 3517–3532. [CrossRef]
15. Manaljav, S.; Farsang, A.; Barta, K.; Tobak, Z.; Juhász, S.; Balling, P.; Babcsányi, I. The impact of soil erosion on the spatial distribution of soil characteristics and potentially toxic element contents in a sloping vineyard in Tállya, Ne Hungary. *J. Environ. Geogr.* **2021**, *14*, 47–57. [CrossRef]
16. Kasim, M.N.; Raheem, A.M. Evaluation of some soil characteristics from field SPT values using random number generation technique. *IOP Conf. Ser. Earth Environ. Sci.* **2021**, *779*, 012017. [CrossRef]
17. Massari, C.; Pellet, V.; Tramblay, Y.; Crow, W.T.; Gründemann, G.J.; Hascoetf, T.; Penna, D.; Modanesi, S.; Brocca, L.; Camici, S.; et al. On the relation between antecedent basin conditions and runoff coefficient for European floods. *J. Hydrol.* **2023**, *625*, 130012. [CrossRef]

18. Cui, Y.; Pan, C. Hydrological responses to litter density on runoff-infiltration patterns and water conservation in *Pinus tabuliformis* plantation. *J. Hydrol.* **2023**, *619*, 129293. [CrossRef]
19. Edokpa, D.; Milledge, D.; Allott, T.; Holden, J.; Shuttleworth, E.; Kay, M.; Johnston, A.; Millin-Chalabi, G.; Scott-Campbell, M.; Chandler, D.; et al. Rainfall intensity and catchment size control storm runoff in a gullied blanket peatland. *J. Hydrol.* **2022**, *609*, 127688. [CrossRef]
20. *GB/T 50095-2014*; Standard for Essential Technical Terms and Symbols in Hydrology. Standardization Administration of China. China Planning Press: Beijing, China, 2014.
21. Hunan Provincial Department of Water Resources. *A Manual for Calculating Rainstorm and Flood in Hunan Province, China*; Hunan Provincial Department of Water Resources: Changsha, China, 2015.
22. Zang, S.; Li, Z.; Zhang, K.; Yao, C.; Liu, Z.; Wang, J.; Huang, Y.; Wang, S. Improving the flood prediction capability of the Xin'anjiang model by formulating a new physics-based routing framework and a key routing parameter estimation method. *J. Hydrol.* **2021**, *603*, 126867. [CrossRef]
23. Tong, B.X.; Li, Z.J.; Yao, C. Estimation of distributed Grid-Xin′anjiang Model parameters based on SoilGrids. *Adv. Water Sci.* **2022**, *33*, 219–226.

Disclaimer/Publisher's Note: The statements, opinions and data contained in all publications are solely those of the individual author(s) and contributor(s) and not of MDPI and/or the editor(s). MDPI and/or the editor(s) disclaim responsibility for any injury to people or property resulting from any ideas, methods, instructions or products referred to in the content.